

## Performance of cold-formed steel wall frames under compression

Chi-Ling Pan<sup>†</sup>

*Department of Construction Engineering, Chaoyang University of Technology, 168, Gifeng E. Rd., Wufeng, Taichung County, Taiwan, R.O.C.*

Jui-Lin Peng<sup>‡</sup>

*Department of Construction Engineering, National Yunlin University of Science & Technology, 123, Section 3, University Road, Touliu, Yunlin, Taiwan, R.O.C.*

*(Received September 10, 2004, Accepted March 30, 2005)*

**Abstract.** This study presents the strength of braced and unbraced cold-formed steel wall frames consisting of several wall studs acting as columns, top and bottom tracks, and bracing members. The strength and the buckling mode of steel wall frames were found to be different due to the change of bracing type. In addition, the spacing of wall studs is a crucial factor to the strength of steel wall frames. The comparisons were made between the test results and the predictions computed based on AISI Code. The related specifications do not clearly provide the effective length factors for the member of cold-formed steel frame under compression. This paper proposes effective length factors for the steel wall frames based on the test results. A theoretical model is also derived to obtain the modulus of elastic support provided by the bracing at mid-height of steel wall frames in this research.

**Key words:** cold-formed steel; wall frame; channel bridging; strap bracing; effective length factor.

---

### 1. Introduction

In light-weight building construction, cold-formed steel wall frame is the major structural element to carry axial and lateral loadings. The cold-formed steel framing system consists of wall studs acting as columns, top and bottom tracks, and sheathing material. In addition, the wall sometime is constructed by using the bracings depending on the strength requirement.

In the design of load bearing wall, the support provided by the sheathing material is not considered because the sheathing material is not treated as a structural material. The Australia Standard (1996) only considers the sheathing material to provide lateral and rotational supports to the studs in the plane of the wall. The strength of the wall computed according to the AISI Specification (2001) is depending on the overall buckling of stud, column buckling between wallboard fasteners, and shear strength of the sheathing material.

---

<sup>†</sup>Associate Professor, Corresponding author, E-mail: [clpan@mail.cyut.edu.tw](mailto:clpan@mail.cyut.edu.tw)

<sup>‡</sup>Professor

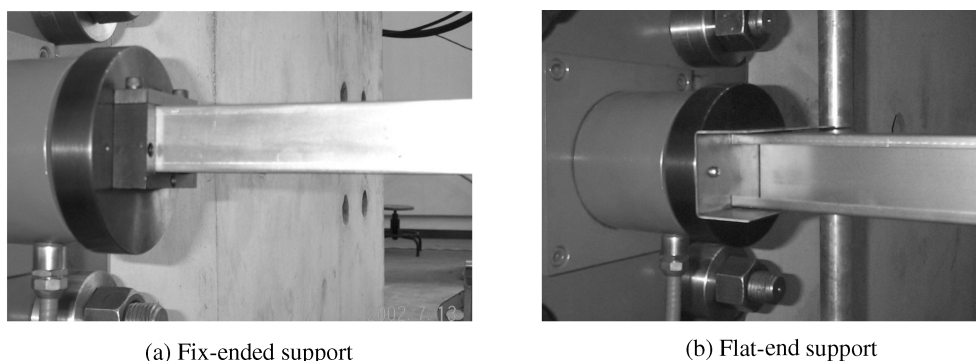


Fig. 1 Photos of support conditions

Simaan and Pekoz (1976) derived an analytical formulation of the steel stud performance considering the bracing action of the wallboard which was usually referred to as diaphragm bracing. Miller and Pekoz (1993) conducted tests to study the performance of cold-formed steel wall studs. The effect of mid-height strap bracing and channel bridging are also evaluated. Based on the test results, the effective lengths factors of unbraced flat-end wall studs are recommended to be  $K_x = K_y = K_t = 0.65$ , and the effective length factors of braced flat-end wall studs are recommended to be  $K_x = 0.65$ ,  $K_y = 0.4$ , and  $K_t = 0.4$ . A research conducted by Miller and Pekoz (1994a) concluded that the experimental results contradict the shear-diaphragm model, as applied to gypsum-sheathed wall studs, assumed by AISI Specification. Contrary to the shear-diaphragm model, the strength of gypsum wallboard braced studs was observed to be rather insensitive to stud spacing. Telue and Mahendran (2001) studied the wall frames lined with and without plasterboard. They concluded that (1) the failure loads of the studs in an unlined wall frame can be approximately predicted by the AS and AISI methods and using effective length factors of  $K_x = K_y = K_t = 0.75$ ; (2) both the AS and AISI methods can predict the failure loads of studs lined on both sides if the effective length factors  $K_x$ ,  $K_y$ , and  $K_t$  are taken as 0.75, 0.1, and 0.1, respectively; (3) the design methods are inadequate in predicting the failure loads of the studs lined on one side; (4) any improvement to local buckling behavior can be ignored for the lined wall frames.

Pan and Chung (2004) investigated the axial-loading behaviors of C-shaped sections with or without web openings. Two different end conditions – fixed-end condition and flat-end condition simulating the wall stud installation were adopted in the column tests as shown in Fig. 1(a) and Fig. 1(b), respectively. The lengths of specimens were designed to be 3.5 m. The torsional-flexural buckling was found in all the specimens. The test results showed that the channel sections with a nominal overall web width of 65 mm, nominal overall flange width of 45 mm, and nominal lip width of 10 mm had similar ultimate strengths for two different end conditions. It was concluded that the effective length factors of flat-end studs without any bracing were recommended to be  $K_x = 0.5$ ,  $K_y = 0.5$ , and  $K_t = 0.5$ .

## 2. Experimental study

The test material used in this study is SSC400 sheet steel specified in Chinese National Standard (1994) with a nominal ultimate tensile strength of 400 N/mm<sup>2</sup> (41 kgf/mm<sup>2</sup>) and up. The 2.3 mm-thick sheet steel was used to fabricate the specimens. The material properties of steel were obtained by tensile coupon tests. The yield stress and tensile strength of steel are 297.25 MPa and 361.23 MPa, respectively.

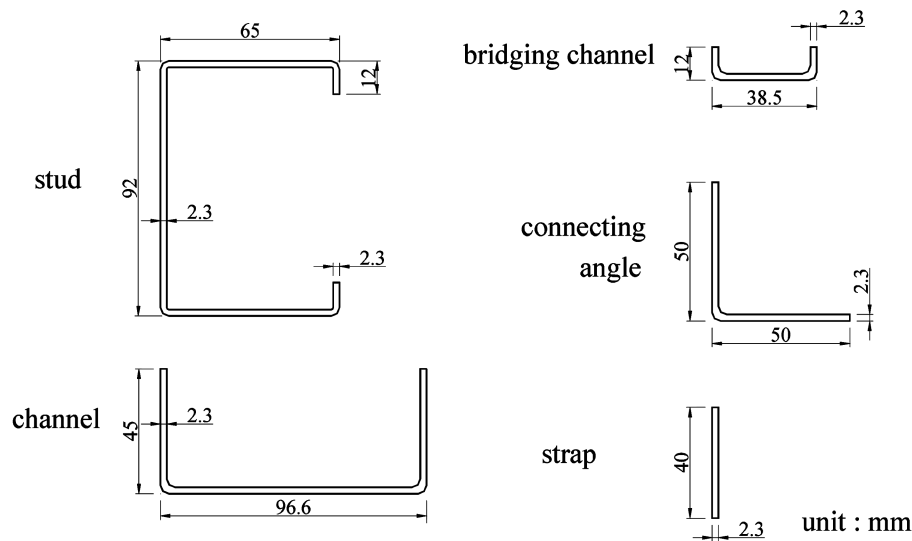


Fig. 2 Dimensions of sections

Due to the dimension of wallboard, the height of cold-formed steel wall frame conducted by most researchers were limited to be around 2.4 m. Different from the regular size of wall studs used in the residential construction, the height of steel wall frames was selected to be 3.0 m in this study. In addition, a thicker thickness of 2.3 mm was chosen for the steel wall studs in order to consider the utilization of high wind and high seismic areas. Three different stud spacing, 20 cm, 40 cm, and 60 cm, were also investigated for the frame tests. A total of 18 cold-formed steel wall frames with bracings at mid-height was investigated in this research.

### 2.1. Specimens

According to the findings by Sheikh, Kassas, and Mackie (2001), the wall studs have better load-carrying capacity when the overall width to depth ratios equal to 0.7 for the sections having same cross-sectional areas. The C-shaped section with a nominal overall web depth of 92 mm, nominal overall flange width of 65 mm, and nominal lip width of 12 mm was chosen to be the wall stud in this study. The length of studs is designed to be 3.0 m. The web perforations are 39 mm×39 mm square hole with 500 mm spacing for all specimens. Fig. 2 shows the dimensions of sections used in the steel wall frames. In order to study the effect of bracing to the wall frames, two types of bracings – channel bridging and strap bracing were adopted in the tests. Details of two types of bracing, strap bracing and channel bridging, can be referred to Fig. 3 and Fig. 4, respectively.

### 2.2. Test setup

Prior to the wall framing testing, individual column tests were conducted to study overall buckling behavior. A compressive testing machine with a capacity of 98 kN was used to conduct all the column tests. The configuration of test setup is shown in Fig. 5. The flat-end support was used for the end conditions of column tests. During the tests, a LVDT (Linear Variable Differential Transformer) was

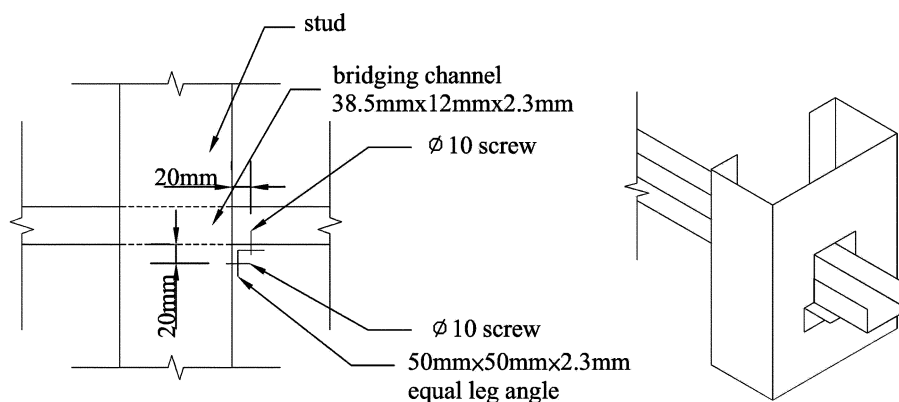


Fig. 3 Details of channel bridging

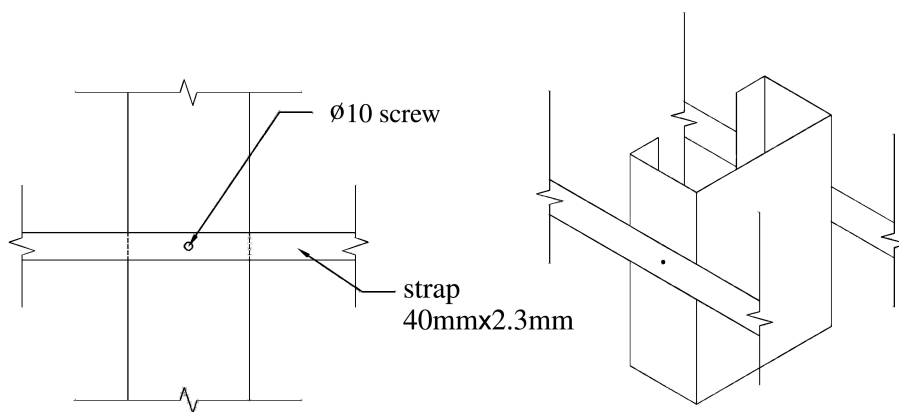


Fig. 4 Details of strap bracing

used to measure the axial deformation for each specimen. All steel wall frames tests were performed by using a 1300-kN test system as shown in Fig. 6. Strain gauges were also attached on the surfaces of specimens to monitor the strain variations throughout the test. In order to obtain good test results, a small amount of preload (about 5% of the ultimate load) was applied on the wall frame for the purpose of checking the alignment of the frame prior to the test.

### 2.3. Test results

A total of 18 steel wall frame tests and 3 long-column tests were conducted in this investigation. As expected, the torsional-flexural buckling behavior was observed for 3 column tests. The ultimate loads of these three individual column tests are 63.87 kN, 59.42 kN, and 58.21 kN. An average ultimate load of 60.50 kN was obtained from the long-column tests. The torsional-flexural buckling behavior was also found for the steel wall frames with channel bridging bracing as shown in Fig. 7. A different buckling behavior – flexural buckling was observed for most steel wall frames with strap bracing. As shown in Fig. 8, the steel straps were observed to have an S-type deformation as the strength of wall frame reaching the ultimate. The average tested ultimate loads of wall frames are presented in Table 1.

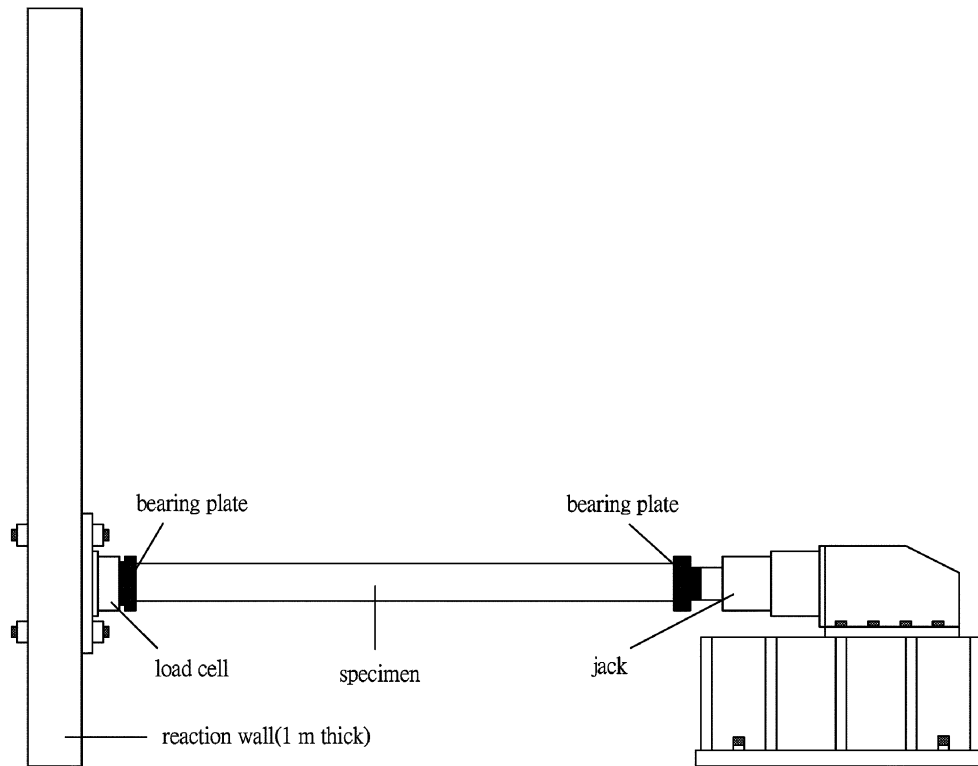


Fig. 5 Setup of the column tests

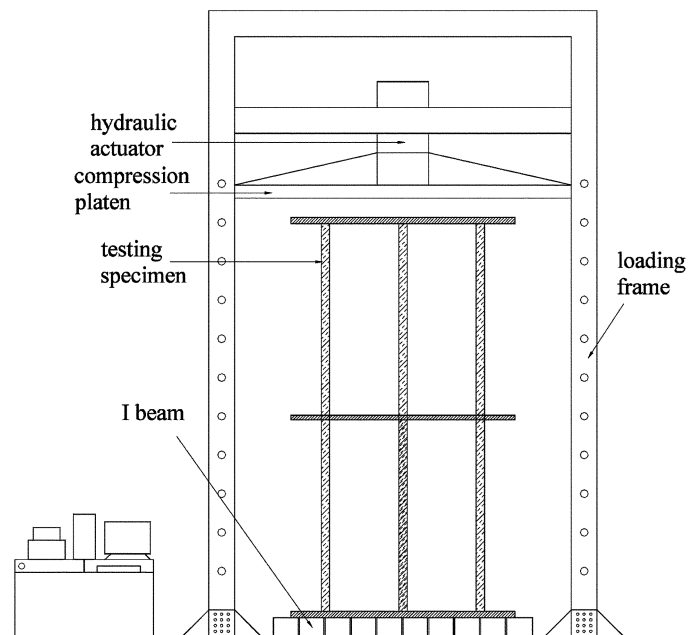


Fig. 6 Setup of the steel wall framing tests



Fig. 7 Typical failure type of wall frames with channel bridging

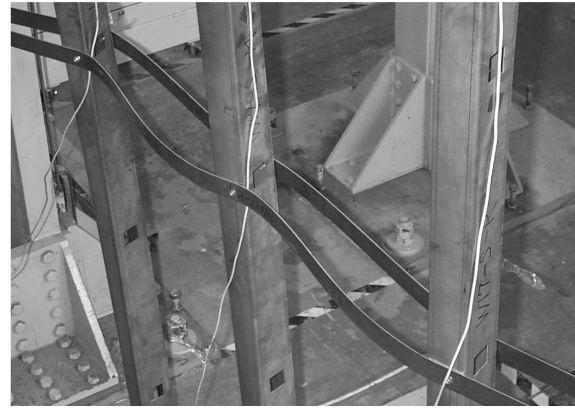


Fig. 8 S-type deformation of strap bracing

Table 1 Average tested ultimate loads of wall frames

Specimen	Average ultimate load of frame $P_{ult}$ (kN)	Average stud load $P_{test}$ (kN)	Specimen	Average ultimate load of frame $P_{ult}$ (kN)	Average stud load $P_{test}$ (kN)
F20B	195.99	65.33	F20S	236.44	78.81
F40B	217.83	72.61	F40S	216.05	72.02
F60B	196.84	65.61	F60S	204.78	68.26

Note: In the designation of specimen, 20, 40, 60 represent the stud spacing.  
B and S represent the channel bridging and strap bracing, respectively.

### 3. Evaluation of experimental data

#### 3.1. Long-column tests

Only uniformly compressed stiffened element with circular hole is provided to compute the effective area of the section in the AISI specification. These design recommendations are mainly based on the testing of cold-formed steel columns with circular holes presented by Qrtiz-Colberg (1981). Therefore, a simplified approach proposed by Miller and Pekoz (1994b) was adopted to calculate the strengths of the specimens with rectangular web perforations in this study. The method uses a simple modification of the unified effective width approach already applied to cold-formed steel sections. The web is modeled as two unstiffened elements, one on either side of the perforation, thus replacing the stiffened element present without perforation. The approach consists of the following:

$$\text{If } (w - b) > W_p \quad (1)$$

then  $w-b$  determines the ineffective portion of the web,

$$\text{If } (w - b) \leq W_p \quad (2)$$

then  $W_p$  determines the ineffective portion of the web,

where  $w$  = flat width of the web;  $b$  = effective width of the web ignoring the perforations; and  $W_p$  = width of the perforation.

In addition, the effective length is not specified for the column with flat-end condition in the AISI specification. It was found that the strength of individual long-column (unbraced) predicted by adopting AISI and AS/NZS specifications and using  $K_x = K_y = K_t = 1.0$  seems conservative. By applying  $K_x = 0.65$ ,  $K_y = 0.5$ , and  $K_t = 0.5$  as well as the method of calculating rectangular web perforations mentioned previously in the calculation of strength of columns in this study, good agreement can be obtained with the test results.

### 3.2. Wall frames tests

It was observed from Table 1 that the average stud loads of the frames with bracing at mid-height are larger than the average ultimate load of individual columns (60.50 kN). Table 2 lists the tested stud loads for the wall frames with channel bridging and strap bracing. The tested stud load ( $P_{test}$ ) listed in Table 2 is calculated by dividing the tested ultimate load of wall frame by three. The tested ultimate loads of the frames using strap bracing are larger than those using channel bridging for the wall frames having same stud spacing for most specimens. It was also noted that the percentage increases in average ultimate load due to the decrease in stud spacing are approximately the same for the steel wall frames

Table 2 Comparison of tested stud loads and computed resistances of wall frames

Bracing type (1)	Spec. No. (2)	$P_{test}$ (kN) (3)	$P_{comp}$ (kN) (4)	$P_{test}/P_{comp}$ (5)
Channel bridging	F20B-1	65.61	65.67	0.999
	F20B-2	65.44	65.58	0.998
	F20B-3	64.93	64.98	0.999
	F40B-1	70.53	64.95	1.086
	F40B-2	74.52	65.37	1.140
	F40B-3	72.79	65.02	1.119
	F60B-1	67.13	65.19	1.030
	F60B-2	N/A	65.42	N/A
	F60B-3	64.10	65.34	0.981
mean				1.044
S.D.				0.062
Strap bracing	F20S-1	81.17	78.09	1.039
	F20S-2	80.35	78.30	1.026
	F20S-3	74.93	78.13	0.959
	F40S-1	71.04	71.63	0.992
	F40S-2	74.22	71.79	1.034
	F40S-3	70.80	71.79	0.986
	F60S-1	N/A	65.23	N/A
	F60S-2	69.64	65.00	1.071
	F60S-3	66.88	65.41	1.022
mean				1.016
S.D.				0.035

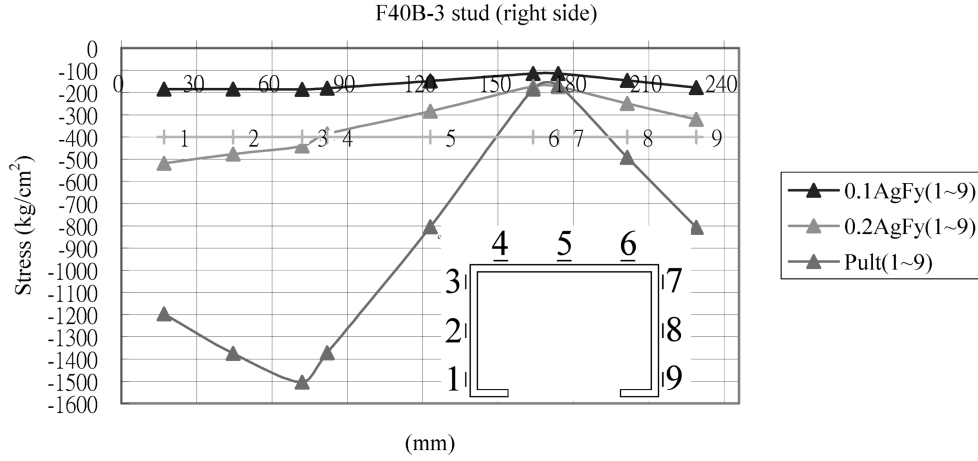


Fig. 9 Strain gauge readings of the stud in Specimen F40B-3

with strap bracing. However, this phenomenon was not observed in the wall frames with channel bridging. The steel straps were observed to have an S-type deformation as the strength of wall frame reaching the ultimate. It is possibly because the strap bracing provides better rotational restraint for the steel wall frame. And this is why the failure mode for wall frames with channel bridging are found to be torsional-flexural buckling, which is same type of failure mode obtained in individual column test, instead of flexural buckling for frames with strap bracing.

Fig. 9 shows the strain gauge readings in the cross section of Specimen F40B-3 at three different loading stages –  $0.1 A_g F_y$ ,  $0.2 A_g F_y$ , and  $P_{ult}$ . The placements of strain gauges are also shown in Fig. 9. The cross section mounted the strain gauges is located at the upper  $1/4$  length of stud where is 75 cm from top end of stud. It was observed from Fig. 9 that the compressive stresses are distributed in entire section during three loading stages. Due to one axis of symmetry, the failure mode of torsional-flexural buckling normally can be found for the channel section under compression. The axial stresses in the cross section of a channel stud are depends on the amount of flexural, torsional, and compressive stresses at failure mode. The axial stress at the section can be determined by applied the theoretical equation (Eq. (3)). Fig. 10 shows the schematic plots of stress distribution for the channel stud with torsional-flexural buckling behavior. The stress distribution of the cross section reaching the ultimate shown in Fig. 9 can be well described by observing Fig. 10.

$$\sigma = \frac{P}{A} + \frac{M_{xy}}{I_x} - \frac{M_{yx}}{I_y} + E \omega_n \phi'' \quad (3)$$

In the calculation of wall studs in compression listed in the AISI specification (2001), the effective length factors used in computing  $\sigma_{ex}$ ,  $\sigma_{ey}$ , and  $\sigma_t$  are assumed to be 1.0. It seems that the strengths computed by using the same assumption are underestimated as comparing with the tested values of the steel wall frames (braced at mid-height). For computing the stud strengths of wall frames tested in this study, it is concluded that the effective length factors  $K_x = 0.65$ ,  $K_y = 0.4$ , and  $K_t = 0.4$  provide best fit to the tested values as adopting the calculating procedure listed in the AISI specification (2001). The simplified approach method proposed by Miller and Pekoz (1994b) was used to calculate the effective



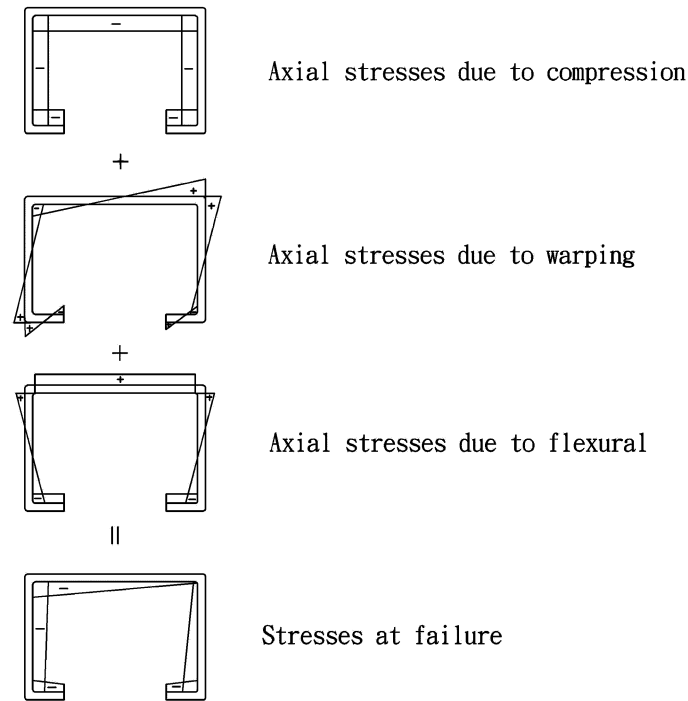


Fig. 10 Schematic plots of stress distribution for the channel stud with torsional-flexural buckling behavior

cross-sectional properties of wall studs the same as that used in the analysis of individual columns. Comparisons of the computed stud strengths and the tested values are listed in Table 2. The tested stud loads are listed in column (3) of Table 2. By considering effective length factors  $K_x = 0.65$ ,  $K_y = 0.4$ , and  $K_t = 0.4$ , the computed stud strength of each specimen is listed in column (4) of Table 2, while the computed values for the strap-bracing frames were obtained by multiplying a factor of  $Q$  as listed in Eq. (4) shown as follows:

$$Q = 1.3 - 0.005 \times S \quad (4)$$

where  $S$  = wall stud spacing

It was found that the tested stud loads for the wall frames with channel bridging are not proportional to the change of stud spacing. From conservative point of view, the computed values for the channel-bridging frames were calculated by applied effective length factors  $K_x = 0.65$ ,  $K_y = 0.4$ , and  $K_t = 0.4$  only. The mean values and standard deviations of  $P_{test}/P_{comp}$  are (1.044 and 0.062) for frames with channel bridging and (1.016 and 0.035) for frames with strap bracing.

#### 4. Analytical model of steel wall frame

In order to investigate the effect of bracing on the strength of wall frames, bracings at mid-height of studs were studied in this research. In analyses, the restraints provided by the straps to the stud can be modified as elastic springs in the  $x$  and  $y$  directions, as well as a rotational spring in the  $z$  axis (parallel

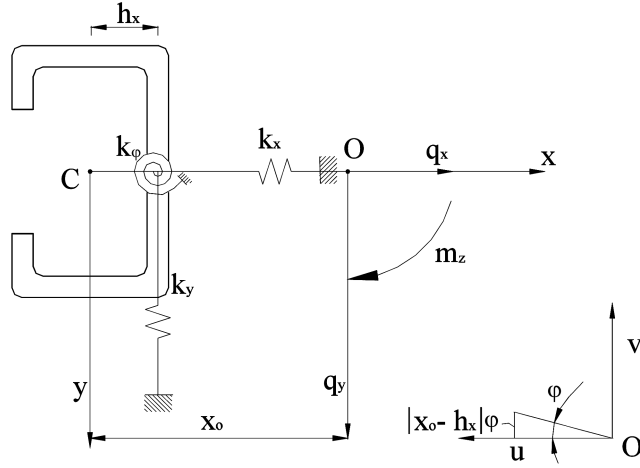


Fig. 11 Simplified restraint model for thin wall member

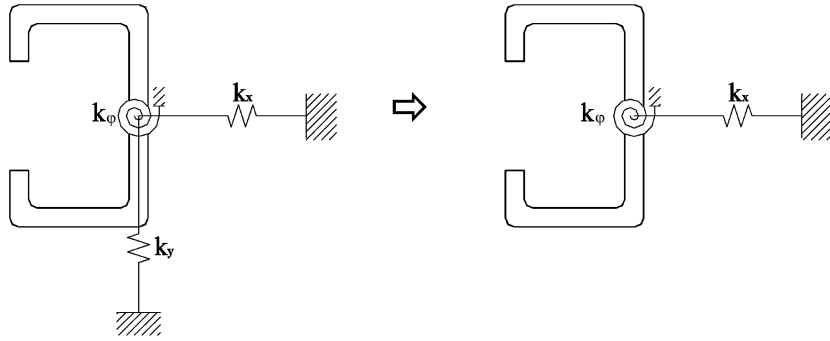


Fig. 12 Restraint model in analysis

to the axis of the stud). Even though it was observed from the test results that the less rotational restraints are provided by the channel bridging, the rotational spring is also adopted in the analytical model of the stud with channel bridging for comparison purpose. Two flat-end supports of wall frame were assumed to be fixed.

In the formulation of differential equations for the wall frame, a model was adopted on the basis of the concept provided by Timoshenko and Gere (1961). This model considers the stability of a centrally compressed bar which is supported elastically throughout its length in such a way that lateral reactions proportional to the deflection will develop during buckling. Taking advantage of one axis of symmetry, the model can be simplified as Fig. 11. And the differential equations of equilibrium are listed as Eqs. (5), (6), and (7).

$$EI_y \frac{d^4 u}{dz^4} + P \frac{d^2 u}{dz^2} + k_x u = 0 \quad (5)$$

$$EI_x \frac{d^4 v}{dz^4} + P \left( \frac{d^2 v}{dz^2} - x_o \frac{d^2 \phi}{dz^2} \right) + k_y [v - (x_o - h_x) \phi] = 0 \quad (6)$$

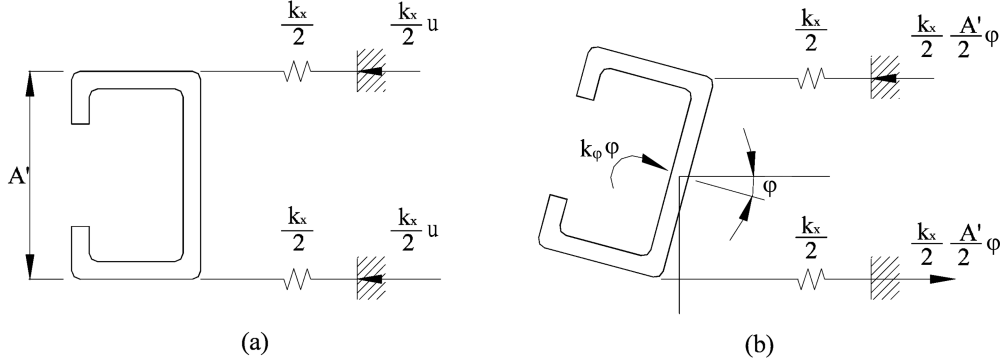


Fig. 13 Axial spring instead of rotational spring in analysis

$$C_1 \frac{d^4 \varphi}{dz^4} - (C - I_o P / A) \frac{d^2 \varphi}{dz^2} - P x_o \frac{d^2 v}{dz^2} - k_y [v - (x_o - h_x) \varphi] (x_o - h_x) + k_\varphi \varphi = 0 \quad (7)$$

where  $u$  = deflection in the  $x$  direction;  $v$  = deflection in the  $y$  direction;  $\varphi$  = rotational angle in the  $z$  direction;  $A$  = cross-sectional area;  $I_x$  = moment of inertia to the  $x$ -axis;  $I_y$  = moment of inertia to  $y$ -axis;  $I_o$  = polar moment of inertia about the shear center;  $C$  = torsional rigidity ( $=GJ$ );  $C_1$  = warping rigidity ( $=EC_w$ ).

It is observed from the tests that the deflections in the  $y$  direction are quite large as compared to the deflections in the  $x$  direction. It is assumed that the stiffness provided by the  $y$ -direction spring can be ignored as shown in Fig. 12. Following the model suggested by Lee and Miller (2001), the torsional modulus of the elastic support ( $k_\varphi$ ) is represented in terms of the rigidity of the elastic support in the  $x$  direction, that means the rotational spring is replaced by two axial springs as shown in Fig. 13.

Based on the model shown in Fig. 13, two  $x$ -direction spring forces ( $F_c$  and  $F_t$ ) can be derived as follows:

$$F_c = -\frac{k_x}{2} \left[ \frac{A'}{2} \sin \varphi + \sqrt{(m\varphi)^2 - (m \sin \varphi)^2} \right] \quad (8)$$

$$F_t = \frac{k_x}{2} \left[ \frac{A'}{2} \sin \varphi + \sqrt{(m\varphi)^2 - (m \sin \varphi)^2} \right] \quad (9)$$

where  $m$  = distance between the shear center and the centerline of the web;  $A'$  = the outside width of the web.

Since  $\varphi$  is small in practice,  $\sin \varphi$  can be substitute to be  $\varphi$ . Therefore, Eqs. (8) and (9) can be simplified as follows:

$$F_c = -\frac{k_x}{2} \left( \frac{A'}{2} \varphi \right) \quad (10)$$

$$F_t = \frac{k_x}{2} \left( \frac{A'}{2} \varphi \right) \quad (11)$$

By using Eqs. (10) and (11), the torsional modulus of elastic support ( $k_\varphi$ ) can be represented as  $k_x(A')^2/4$ . Assuming the mode shape equations  $u = A_1 \sin(n\pi z/L)$ ,  $v = A_2 \sin(n\pi z/L)$ , and  $\varphi = A_3 \sin(n\pi z/L)$

that satisfy the boundary conditions, Eqs. (5), (6), and (7) can be rewritten as follows:

$$EI_y \left( \frac{n\pi}{L} \right)^4 - P \left( \frac{n\pi}{L} \right)^2 + k_x = 0 \quad (12)$$

$$EI_x A_2 \left( \frac{n\pi}{L} \right)^4 - P \left( A_2 \left( \frac{n\pi}{L} \right)^2 - x_o A_3 \left( \frac{n\pi}{L} \right)^2 \right) = 0 \quad (13)$$

$$C_1 A_3 \left( \frac{n\pi}{L} \right)^4 + \left( C - I_o \frac{P}{A} \right) A_3 \left( \frac{n\pi}{L} \right)^2 + P x_o A_2 \left( \frac{n\pi}{L} \right)^2 + \frac{k_x}{4} (A')^2 A_3 = 0 \quad (14)$$

Therefore, the flexural buckling strength can be obtained by solving Eq. (12), and listed as follows:

$$P_f = \frac{\pi^2 EI_y}{L^2} \left( n^2 + \frac{L^4 k_x}{n^2 \pi^4 EI_y} \right) \quad (15)$$

And by using Eqs. (13) and (14), the torsional-flexural buckling strength can be derived as below:

$$\det \begin{vmatrix} EI_x \left( \frac{n\pi}{L} \right)^4 - P_{tf} \left( \frac{n\pi}{L} \right)^2 & P_{tf} x_o \left( \frac{n\pi}{L} \right)^2 \\ P_{tf} x_o \left( \frac{n\pi}{L} \right)^2 & C_1 \left( \frac{n\pi}{L} \right)^4 + \left( C - \frac{I_o}{A} P_{tf} \right) \left( \frac{n\pi}{L} \right)^2 + \frac{k_x}{4} (A')^2 \end{vmatrix} = 0 \quad (16)$$

In the analysis of cold-formed steel column, local buckling should be allowed for probably as it tends to reduce the axial-loading strength. Since the stud length using in this study is quite large (3.0 m), the stresses found in the cross section of the stud at the load reaching the maximum are less than the critical local buckling stress. It seems that Eqs. (15) and (16) can be adopted to obtain the modulus of elastic support provided by the bracing at mid-height of steel wall frames in this research. Based on the tested

Table 3 Elastic supports provided by the bracing at mid-height of steel studs

Cross section of stud	Bracing type (spacing)	Spring constant	
92 mm×65 mm×12 mm <i>t</i> = 2.3 mm	Channel bridging (20 cm)	<i>k<sub>x</sub></i> (kN/mm)	0.0021
		<i>k<sub>φ</sub></i> (kN-mm/rad)	4.4002
	Channel bridging (40 cm)	<i>k<sub>x</sub></i> (kN/mm)	0.0026
		<i>k<sub>φ</sub></i> (kN-mm/rad)	5.5664
	Channel bridging (60 cm)	<i>k<sub>x</sub></i> (kN/mm)	0.0021
		<i>k<sub>φ</sub></i> (kN-mm/rad)	4.3022
	Strap bracing (20 cm)	<i>k<sub>x</sub></i> (kN/mm)	0.0033
		<i>k<sub>φ</sub></i> (kN-mm/rad)	6.9580
	Strap bracing (40 cm)	<i>k<sub>x</sub></i> (kN/mm)	0.0025
		<i>k<sub>φ</sub></i> (kN-mm/rad)	5.4390
	Strap bracing (60 cm)	<i>k<sub>x</sub></i> (kN/mm)	0.0023
		<i>k<sub>φ</sub></i> (kN-mm/rad)	4.7530

values, the elastic supports provided by the bracing at mid-height of steel studs are presented in Table 3. The elastic springs in the  $x$  direction ( $k_x$ ) and the rotational springs in the  $z$  axis ( $k_\phi$ ) ranged from 0.0021 to 0.0033 kN/mm and from 4.3022 to 6.9580 kN-mm/rad, respectively.

## 5. Conclusions

This study primarily presents the experimental determination of the strength of cold-formed steel wall frames with or without bracing. Eighteen steel frames and three individual columns were tested in this study. Based on the test results, the following conclusions can be made:

1. The effective length is not specified for the flat-ended column in the AISI specification. It was found that individual long-column strength (unbraced) predicted by adopting AISI specification and using  $K_x = K_y = K_t = 1.0$  seems conservative. By applying  $K_x = 0.65$ ,  $K_y = 0.5$ , and  $K_t = 0.5$  as well as the method of calculating rectangular web perforations based on the simplified approach method proposed by Miller and Pekoz (1994b), good agreement can be obtained with the test results.
2. The average stud loads of the frames with bracing at mid-height are larger than the average ultimate load of individual columns. The tested ultimate loads of the frames using strap bracing are larger than those using channel bridging for the wall frames having same stud spacing for most specimens.
3. The percentage increases in average ultimate load due to the decrease in stud spacing are approximately identical for the steel wall frames with strap bracing. However, this phenomenon was not observed in the wall frames with channel bridging. It is possibly due to the strap bracing provides better rotational restraint for the steel wall frame.
4. For computing the average stud strength of wall frames, it is suggested that the effective length factors  $K_x = 0.65$ ,  $K_y = 0.4$ , and  $K_t = 0.4$  provided best fit to the tested values as adopting the calculating procedure listed in the AISI specification. Same as that used in the analysis of individual columns, the simplified approach method proposed by Miller and Pekoz (1994b) was used to calculate the effective cross-sectional properties of wall studs.
5. It was found that the tested values of steel wall frames with strap bracing were affected by the stud spacing. The calculated values for the strap-bracing frames can be improved by multiplied a factor of  $Q$  as listed in Eq. (4).
6. The stresses found in the studs of steel frames at the load reaching the maximum are less than the critical local buckling stress. A theoretical model derived in this study (Eqs. (15) and (16)) seems can be utilized to obtain the modulus of elastic support provided by the bracing at mid-height of steel wall frames in this research.

## References

- American Iron and steel Institute (2001), *Specification for the Design of Cold-Formed Steel Structural Members*, Washington, DC.
- American Iron and steel Institute (1986), *Specification for the Design of Cold-Formed Steel Structural Members*, Washington, DC.
- El-Sheikh, A.I., El-Kassas, E.M.A., and Mackie, R.I. (2001), "Performance of stiffened and unstiffened cold-formed channel member in axial compression", *Eng. Struct.*, **23**, 1221-1231.

- Lee, Y.K. and Miller, T.H. (2001), "Axial strength determination for gypsum-sheathed cold-formed steel wall stud composite panels", *J. Struct. Eng.*, ASCE, **127**(6), 608-615.
- Miller, T.H. and Pekoz, T. (1993), "Behavior of cold-formed steel wall stud assemblies", *J. Struct. Eng.*, ASCE, **119**(2), 641-651.
- Miller, T.H. and Pekoz, T. (1994a), "Behavior of gypsum-sheathed cold-formed steel wall studs", *J. Struct. Eng.*, ASCE, **120**(5), 1644-1650.
- Miller, T.H. and Pekoz, T. (1994b), "Unstiffened strip approach for perforated wall studs", *J. Struct. Eng.*, ASCE, **120**(2), 410-421.
- Ortiz-Collberg, R.A. (1981), "The load carrying capacity of perforated steel columns", MS Thesis, Cornell Univ., Ithaca, N.Y.
- Pan, C.L. and Chung, P.T. (2004), "The compressive behavior of C-shaped cold-formed steel members with web openings", *The 7th Nat. Conf. on Structure Engineering*, Chung-Li, Taiwan, R.O.C.
- Standards Australia (1996). *Cold-formed Steel Structures*, AS/NZS 4600, Sydney.
- Simaan, A and Pekoz, T. (1976), "Diaphragm braced members and design of wall studs", *J. Struct. Div.*, ASCE Proceeding, **102**(1), 77-93.
- Telue, Y. and Mahendran, M. (2001), "Behaviour of cold-formed steel wall frames lined with plasterboard", *J. Constructional Steel Research*, Elsevier Science Ltd, **57**, 435-452.
- Timoshenko, S.P. and Gere, J.M. (1961). *Theory of Elastic Stability*, 2nd Edition, McGraw-Hill, N.Y.

SC